JACS
JOURNAL OF THE AMERICAN CHEMICAL SOCIETY
Article
pubs.acs.org/JACS
Terms of Use CC-BY

Tunable Porous Organic Crystals: Structural Scope and Adsorption Properties of Nanoporous Steroidal Ureas

Ramalingam Natarajan,[†,#] Lydia Bridgland,[†] Anchalee Sirikulkajorn,[†] Ji-Hun Lee,[†] Mairi F. Haddow,[†] Germinal Magro,[†] Bakhat Ali,[†] Sampriya Narayanan,[†] Peter Strickland,[†] Jonathan P. H. Charmant,[†] A. Guy Orpen,[†] Neil B. McKeown,[‡] C. Grazia Bezzu,[‡] and Anthony P. Davis*[,†]

[†]School of Chemistry, University of Bristol, Bristol, BS8 1TS, United Kingdom
[‡]School of Chemistry, Cardiff University, Cardiff, CF10 3AT, United Kingdom

Supporting Information

ABSTRACT: Previous work has shown that certain steroidal bis-(*N*-phenyl)ureas, derived from cholic acid, form crystals in the $P6_1$ space group with unusually wide unidimensional pores. A key feature of the nanoporous steroidal urea (NPSU) structure is that groups at either end of the steroid are directed into the channels and may in principle be altered without disturbing the crystal packing. Herein we report an expanded study of this system, which increases the structural variety of NPSUs and also examines their inclusion properties. Nineteen new NPSU crystal structures are described, to add to the six which were previously reported. The materials show wide variations in channel size, shape, and chemical nature. Minimum pore diameters vary from ∼0 up to 13.1 Å, while some of the interior surfaces are markedly corrugated. Several variants possess functional groups positioned in the channels with potential to interact with guest molecules. Inclusion studies were performed using a relatively accessible tris-(*N*-phenyl)urea. Solvent removal was possible without crystal degradation, and gas adsorption could be demonstrated. Organic molecules ranging from simple aromatics (e.g., aniline and chlorobenzene) to the much larger squalene (M_w = 411) could be adsorbed from the liquid state, while several dyes were taken up from solutions in ether. Some dyes gave dichroic complexes, implying alignment of the chromophores in the NPSU channels. Notably, these complexes were formed by direct adsorption rather than cocrystallization, emphasizing the unusually robust nature of these organic molecular hosts.

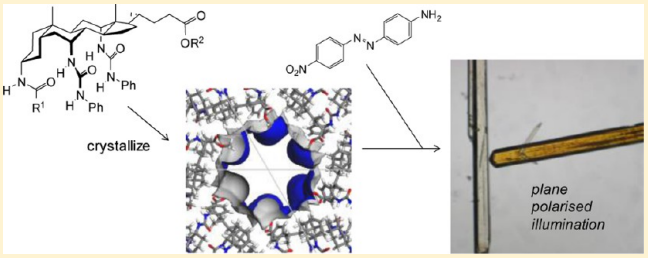

INTRODUCTION

Crystal engineering—the rational design of crystalline molecular solids—remains an important challenge for chemistry.[1] Crystal structure prediction is not yet feasible in all cases,[2] and it is therefore useful to develop motifs which allow families of structures to be generated in a reliable fashion.[3] There is special interest in motifs which lead to microporous (or nanoporous) crystals with voids on the scale of ∼0.5−2 nm, sufficient to accommodate molecular guests. Such materials offer various functionalities, such as inclusion and storage of gases,[4] and other guest molecules,[5] the enhancement of optical properties of included guests,[6] the use of pores as reaction vessels to promote the formation of desired products,[7] and the separation of mixtures[8] including enantiomers from racemates.[9] At the same time, the design of porous crystals presents an intriguing problem. Crystallizing species will usually attempt to maximize contact with each other, thus minimizing any void space. To counter this trend is not straightforward and will often require the construction of specially shaped rigid components or units capable of strong and directional interspecies interactions.

Successful approaches to nanoporous crystal engineering may be divided into two categories. On the one hand are the hybrid organic−inorganic "porous coordination polymers" (PCPs) or "metal−organic frameworks" (MOFs),[4a,10] formed by combining metal ions with rigid multivalent ligands. On the other are purely organic systems, which rely on noncovalent bonding to regulate crystal packing.[11] The organic systems may be further divided into intrinsically and extrinsically porous molecular crystals.[11a] Intrinsically porous crystals are based on molecules with predefined open spaces (macrocycles, cages etc.),[4b−e,5b,7a−c,12] whereas extrinsic porosity results simply from crystal packing. Of these three approaches (hybrid, intrinsic/extrinsic organic), the latter is probably the most challenging as open frameworks must be maintained without the help of powerful directional coordination bonds or preexisting cavities. Some solutions have emerged through serendipity, such as the classic urea inclusion compounds.[13] Others are the result of elegant design and/or exploratory work.[4f−h,5c,d,6,7f,8b,c,14] However most studies in this area yield single, specific host structures. There are few motifs which

Received: June 7, 2013
Published: October 22, 2013

 © 2013 American Chemical Society dx.doi.org/10.1021/ja405701u | J. Am. Chem. Soc. 2013, 135, 16912−16925

generate families of readily accessible nanoporous crystals,[15] allowing tuning of void dimensions and material properties.

The work described in this paper is founded on a serendipitous discovery made a few years ago in the course of our program on anion-binding "cholapods".[16] These powerful receptors combine a rigid steroidal scaffold, derived from cholic acid **1** (Chart 1) with various combinations of H-bond donor groups. Most are reluctant to crystallize but a small subset, represented initially by **2**–**4**, were found to form needles from methyl acetate-water or acetone-water mixtures. All three were subjected to X-ray crystallography, with interesting results.[17] Despite the significant differences between **2**–**4**, the external similarity of the crystals was reflected in the internal structures; the three were isomorphous, with almost identical unit cell dimensions and packing arrangements for the invariant steroidal cores. The packing involved the formation of helices with hexagonal symmetry (space group = $P6_1$), surrounding solvent-filled channels. The arrangement is illustrated in Figure 1, using tris-urea **3** as an example. Individual steroid molecules bind to a single molecule of co-crystallized water through 5 H-bonds (Figure 1a) and stack to form columns (Figure 1b). The columns then pack in a hexagonal arrangement to generate the solvent-filled pores. The orientation of the steroids in the columns is such that the terminal groups (methoxy and NHPh) face into the pores and largely determine the nature of the channel surface. This explains why three quite different molecules can be isostructural. Effectively, the terminal groups can expand into the channel interior without affecting the packing of the columns which maintain the structure. The channels, moreover, are unusually wide. In the case of trifluoroacetamide **2**, the average diameter was found to be 16.4 Å. The average diameter for **3** was only slightly less at 15.7 Å, although the surfaces are more irregular (Figure 2). There is thus substantial room, in principle, both for guest molecules and for terminal groups. Preliminary experiments on **2** implied that guest exchange was possible, at least for certain solvents (MeOAc, Et_2O, toluene). Evacuation lead to partial degradation (evidenced by crazing), but the powder X-ray diffraction (XRD) pattern remained largely unchanged.

Chart 1. Formulae for Cholic Acid 1 and Prototype NPSUs 2–4

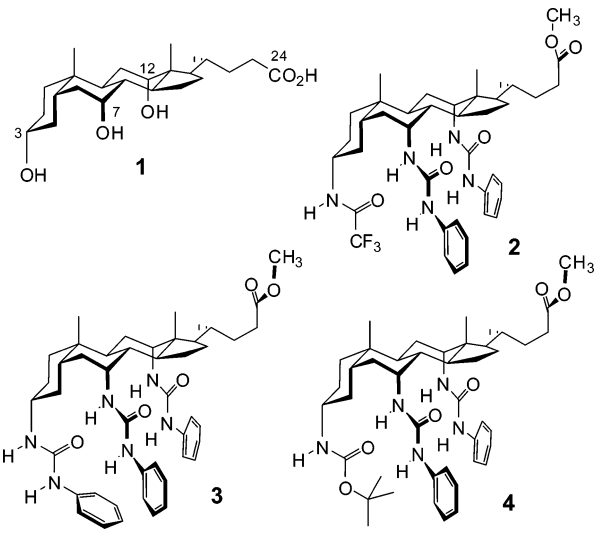

Given the space available within the channels, it seemed likely that a wide range of analogues with a common bis-(*N*-phenylureido)steroidal core (Figure 3) would form crystals isostructural with **2**–**4**. Variation should be feasible not only at the C3 substituent (R^1 in Figure 3) but also at the C24 ester group (R^2 in Figure 3). Moreover as these "nanoporous steroidal ureas" (NPSUs) would be isostructural they should be able to form solid solutions (organic alloys), greatly enlarging the range of systems available. Since our original publication we have confirmed both of these possibilities. We have described a series of three NPSUs with aromatic groups in R^2, and the interesting feature of "water wires" in the channels,[18] and also a range of NPSU-based organic alloys.[19] Herein we provide a more complete description of our work surveying the scope and properties of NPSUs, drawing on 25 examples which have been characterized by X-ray crystallography. We show how the dimensions and shapes of the channels can be tuned, and how their chemical nature can be altered by the introduction of functional groups (including previously unreported alkene and aldehyde functionality). We also report, for the first time, that NPSUs can be porous in the strictest sense, stable to evacuation and capable of gas adsorption. Moreover we show that they can adsorb a remarkable range of guests, including organic dyes with molecular weights up to ∼300 and even the C_{30} hydrocarbon squalene (M_w = 410).

RESULTS AND DISCUSSION

Design and Synthesis. The structures discussed in this paper fall into two groups. The first are esters of 3*α*,7*α*,12*α*-tris-(*N*-phenylureido)-5*β*-cholanoic acid **6** and include **3** as well as the 14 variants **7**–**20** represented in Chart 2. Ester groups R^2 were chosen for variation in size (and thus pore diameter) and surface characteristics (aliphatic vs aromatic vs fluorocarbon) and also to showcase the potential for placing chromophores (e.g., azobenzenes), fluorophores (e.g., pyrenes), and reactive units (e.g., allyl groups) in the channels. The second group are derivatives of methyl 3*α*-amino-7*α*,12*α*-bis-(*N*-phenylureido)-5*β*-cholanoate **5**, including trifluoroacetamide **2**, carbamate **4**, tris-ureas **21**–**26**, and amides **27**–**29** (Chart 3). Again the variable group (R^1) was used to change steric and surface properties and to introduce chromophores and functional groups. In this case some quite reactive and polar units were included, e.g., the aldehyde in **21** and the NHBoc group in **23**.

The routes to these compounds are summarized in Scheme 1. Key intermediates are amine **5** and tris-*N*-phenylurea **3**. Amine **5** is accessible from cholic acid **1** via a multistep but well-established route in ∼40% overall yield.[17,20] Tris-urea **3** may be prepared from **5** by treatment with phenyl isocyanate or more directly from **1** via methyl 3*α*,7*α*,12*α*-triaminocholanoate.[21] Esters **7**–**20** (Chart 2) are available from **3** via equilibration with lithium alkoxide or hydrolysis to acid **6** followed by O-alkylation or carbodiimide-induced esterification. The derivatives in Chart 3 may be prepared from **5** by treatment with an aryl isocyanate (giving **21**–**26**) or an acylating agent (giving **27**–**29**). The preparations of **9**, **10**, **12**, **14**–**19**, **23**, **26**, and **29** have been reported previously.[18,19,22] Procedures for the remaining compounds in Charts 2 and 3 are given in the Supporting Information.

Crystallography. The steroids in Charts 2 and 3 were crystallized from methyl acetate or acetone, to which small amounts of water had been added, through slow evaporation of the organic solvent. In most cases either solvent system was effective. Other polar solvents, such as methanol or ethanol, or

dx.doi.org/10.1021/ja405701u | J. Am. Chem. Soc. 2013, 135, 16912–16925

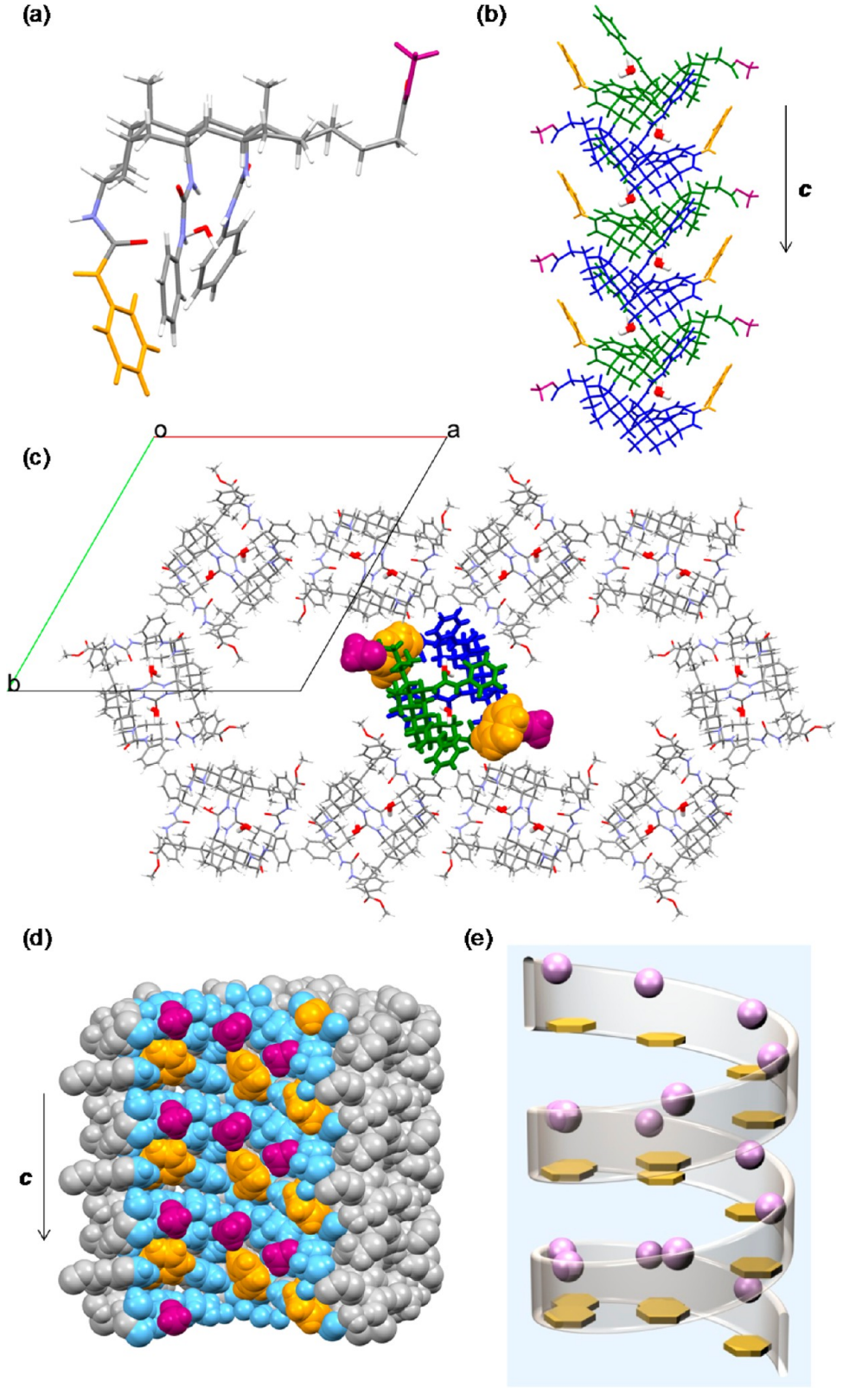

Figure 1. The crystal structure of prototype NPSU **3**. (a) Single molecule of **3** in the crystal. The steroid is solvated by a molecule of water which forms hydrogen bonds to all three urea groups. Terminal OCH_3 and NHPh groups are colored magenta and gold, respectively. (b) Molecules of **3** stack to form columns, running along the crystallographic *c* axis. Representation as for (a) except that core steroidal atoms are colored blue and green in adjacent molecules, and water molecules are shown with thick bonds. (c) The crystal structure viewed down the *c* axis. One column of steroids is highlighted using the coloring from (b), with the OCH_3 and NHPh groups now in spacefilling mode. (d) A single channel sliced in half along the *c* axis, viewed in spacefilling mode. Terminal OCH_3 and NHPh groups retain their coloring, other atoms near or at the internal surface are shown as light blue. (e) 3D schematic representation of a channel, showing helical arrangement of methyl groups and aromatic rings (spheres and hexagons, respectively).

dx.doi.org/10.1021/ja405701u | *J. Am. Chem. Soc.* 2013, 135, 16912−16925

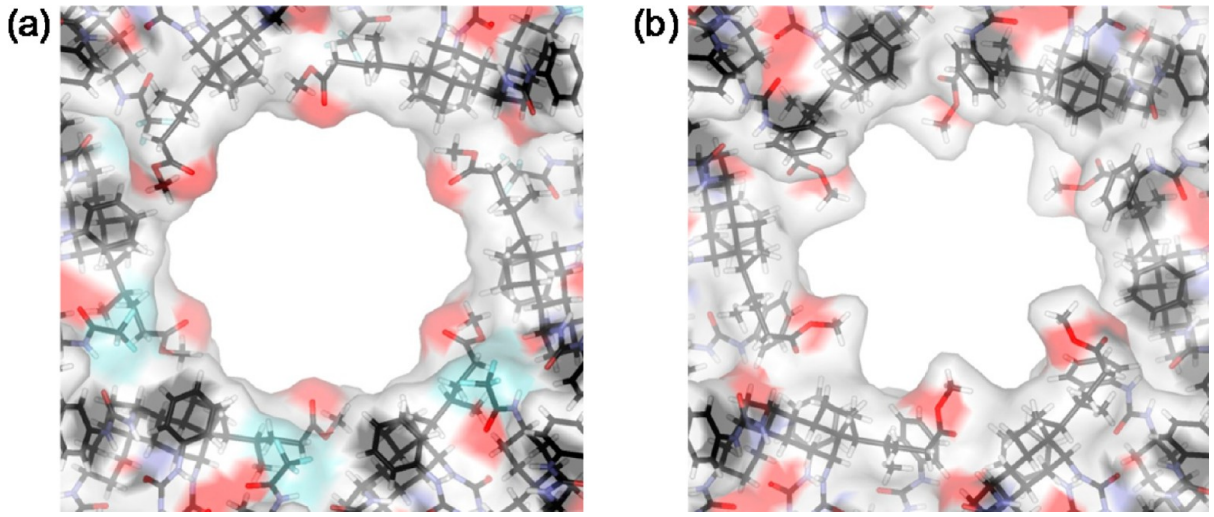

Figure 2. Interior surfaces for trifluoroacetamide **2** and tris-*N*-phenylurea **3** viewed along the *c*-axis. The surfaces were calculated using a 1.4 Å probe.

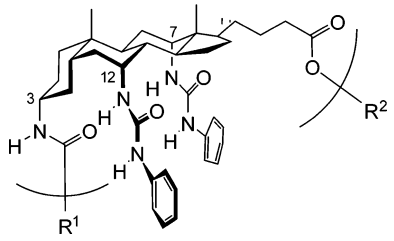

Figure 3. General formula for NPSUs. The core bis-(*N*-phenylureido)-steroidal unit maintains the $P6_1$ nanoporous structure, while groups R^1 and R^2 control the size and nature of the pore.

nonpolar mixtures, such as chloroform-hexane, yielded oils or amorphous solids. All the compounds could be analyzed by single crystal X-ray diffraction (SCXRD), and with the single exception of **29** (see below), all formed crystals with the $P6_1$ NPSU packing. The structures of **2**–**4**, **14**, **16**, and **18** have been reported in communications,[17,18] the remainder are described for the first time herein. Unit cell dimensions for the full series are listed in Table 1. As expected these show only minor variations, the differences between the steroids being accommodated by changes to the shape, diameter, and surface characteristics of the pores. Unsurprisingly, given the open nature of the pore region, disorder in terminal groups R^1 and (especially) R^2 was fairly common, being present in 11 of 25 structures. However, in most cases the groups concerned were divided between just two positions, so that a reasonable model of the crystal (for estimating pore volume etc.) could be obtained by deleting the minor component. This applied to **4**, **8**, **10**, **12**, **13**, and **24** (disorder in R^2), and **22** (disorder in R^1). In two cases, **15** and **19**, deleting one of the two possible positions did not give a viable structure. However, these crystals could be modeled successfully by assuming equal occupancy of both positions, on an alternating basis. After editing where relevant, the smoothed solvent accessible surfaces and resulting guest-accessible volumes were calculated using Materials Studio, employing a probe of radius 1.2 Å. These values are given in Table 1, while images of the surfaces are available as Supporting Information. Also included in Table 1 are minimum pore diameters. These were estimated by repeating the calculation using probes of increasing size until the surface was no longer continuous. The resulting value is, effectively, the

Chart 2. NPSU Structures with Variation of Ester Terminus R^2

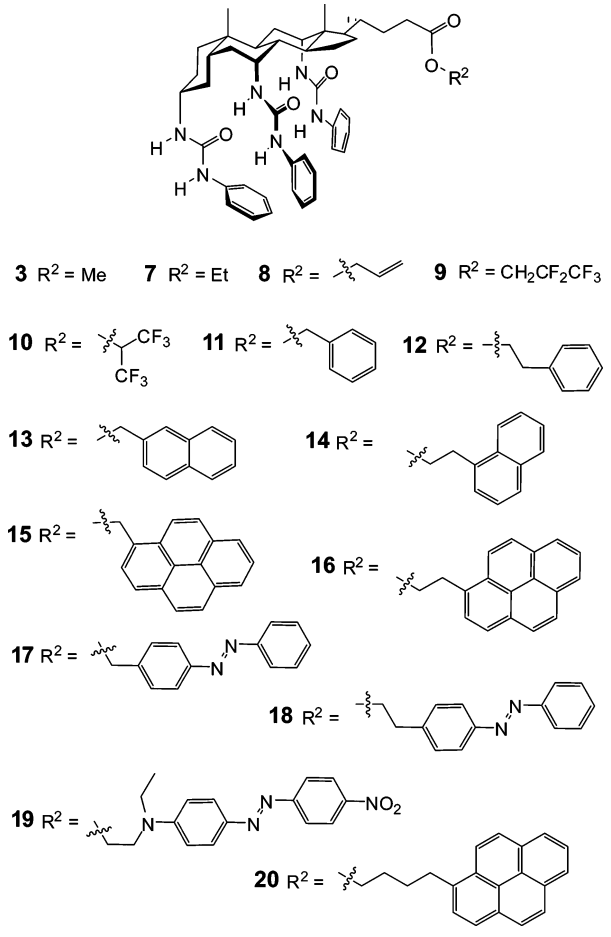

diameter of the largest sphere which can pass through the channel. Images of selected structures viewed down the pores, with terminal groups shown in spacefilling mode, are shown in Figure 4 (compounds from Chart 2, varying ester group R^2) and Figure 5 (compounds from Chart 3, varying C3 terminal group R^1).

dx.doi.org/10.1021/ja405701u | *J. Am. Chem. Soc.* 2013, 135, 16912–16925

Chart 3. NPSU[a] Structures with Variation of C3 Terminal Group R^1

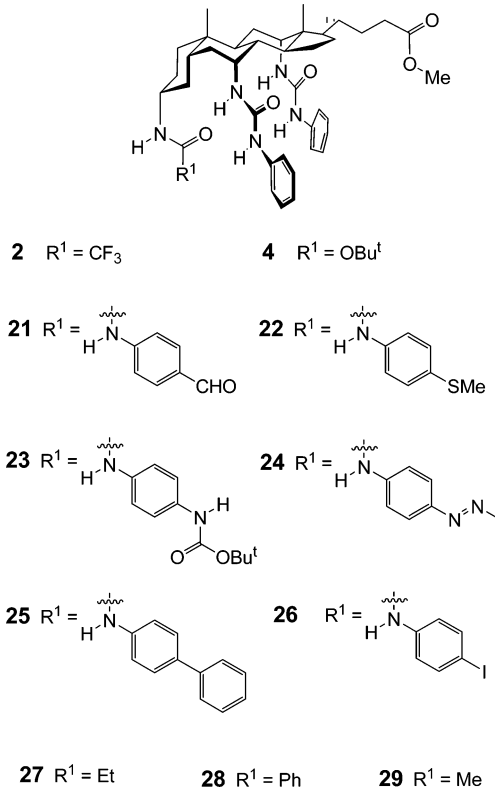

[a]Although **29** is included here for convenience, it does not adopt the NPSU crystal packing. For further details see text.

Table 1 and Figures 4 and 5 illustrate the wide variety of structural properties available via the NPSU system. For example, starting at nearly 20% (for **2**), the volume available in the pores can be tuned downward in small increments essentially to zero (for **15** and **19**). Indeed, by taking advantage of alloy formation,[19] continuous variation should be possible with these compounds. Unsurprisingly, pore volumes and diameters are generally determined by the size of the terminal groups, but more subtle effects are also in play. For example, in the series with varying OR^2 (Chart 2, Figure 4), a 2-carbon spacer between the oxygen and an aromatic group tends to allow efficient packing of the aromatic surface against the side of the channels. Thus, for pyrenyl derivative **16**, space remains down the center for hydrogen-bonded chains of water molecules.[18] In contrast, a 1-carbon methylene spacer directs the aromatic group toward the center of the channel. In the case of pyrenyl derivative **15**, this results effectively in full occupation of the channel; the calculated guest-accessible volume and minimum diameter are both close to zero. Paradoxically, therefore, the larger terminal group (in **16**) leaves more space than the smaller group in **15**.

The shape of the channel wall (smooth vs corrugated) is another feature which can be altered. As mentioned above, compounds for which $R^2 = CH_2CH_2Ar$ (e.g., **14**, **16**, **18**) tend to adopt structures in which the aromatic groups line the surfaces of the channels.[18] The resulting pores are relatively smooth and cylindrical, as illustrated for **14** in Figure 6 (top). In other systems from Chart 2, the channel surface is presumably corrugated, but with random and/or flexible character due to disorder within the crystal. An example is provided by **13**, for which the naphthylmethyl group appears in two orientations, one roughly perpendicular and one more nearly parallel to the channel axis. Well-defined corrugated pores may be accessed by placing extended substituents at R^1 (which is less prone to disorder). Thus for both **24** (R^1 = azobenzene) and **25** (R^1 = biphenyl) the C3-substituent reaches well toward the *c* axis creating strongly asymmetric helical pores (Figure 6, middle and bottom).

This work also shows that the chemical nature of the pore walls can be subject to wide variation. The structures collected in Figures 4 and 5 feature an alkenyl group C=C (**8**), a helical strip of fluorocarbon surface (**10**), an aldehyde (**21**), a thioether (**22**), a Boc-protected amine (**23**), and an

Scheme 1. Synthetic Routes to NPSUs

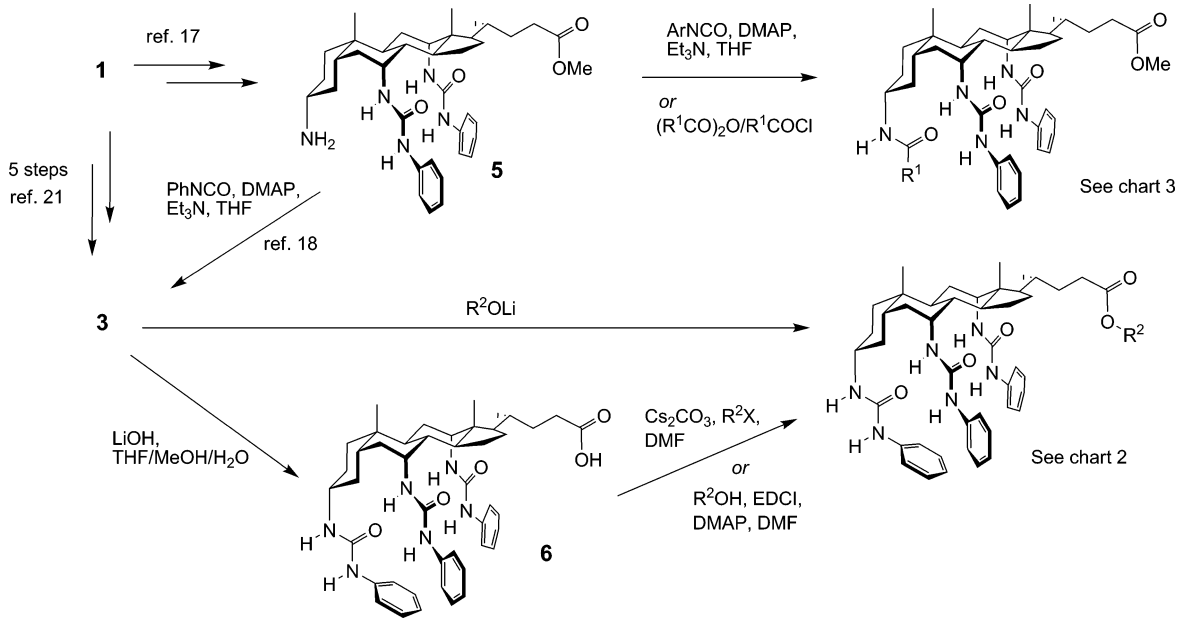

dx.doi.org/10.1021/ja405701u | J. Am. Chem. Soc. 2013, 135, 16912−16925

Table 1. Crystal Data for NPSUs Depicted in Charts 2 and 3

NPSU	$a = b$ (Å)	c (Å)	V (Å^3)	guest accessible volume (Å^3)[a]	guest accessible volume (%)	minimum pore diameter (Å)[b]
2	28.692(4)	11.500(2)	8198(2)	1568.32	19.1	13.1[c]
3	29.0842(6)	11.4888(3)	8416.3(3)	1351.67	16.1	10.8[c]
4	28.834(4)	11.609(2)	8359(2)	1411.22[d]	16.9	10.3[c]
7	28.967(2)	11.5405(18)	8386.3(16)	1136.13	13.5	9.3
8	28.9183(14)	11.5106(6)	8336.3(7)	1037.32[d]	12.4	8.9
9	28.9203(11)	11.5171(4)	8342.2(5)	721.23	8.6	6.6
10	29.0839(7)	11.4442(3)	8383.4(4)	782.17[d]	9.3	7.7
11	28.9611(6)	11.4464(3)	8314.4(3)	704.71	9.6	7.7
12	28.6821(17)	11.3981(8)	8120.5(9)	410.20[d]	5.1	4.9
13	28.9274(6)	11.4568(2)	8302.6(3)	351.01[d]	4.2	4.6
14	28.9480(6)	11.4319(2)	8296.3(3)	239.86	2.9	5.4
15	29.0884(9)	11.3681(8)	8330.2(7)	36.86[e]	0.4	<1.1[f]
16	29.315(3)	11.5430(11)	8590.5(14)	179.33	2.1	5.6
17	29.021(4)	11.4268(15)	8334.7(18)	[g]	–	–
18	29.2924(12)	11.3062(5)	8401.5(6)	119.83	1.4	5.0
19	29.4598(10)	11.4907(4)	8636.5(5)	0.18[e]	0.002	<1.1[f]
20	29.4818(11)	11.4124(4)	8590.4(5)	[g]	–	–
21	28.922(2)	11.4784(11)	8315.3(12)	1133.91	13.6	10.2
22	28.772(4)	11.482(2)	8232(2)	954.12[h]	11.6	9.7
23	29.1996(10)	11.3965(4)	8415.0(5)	475.39	5.6	6.6
24	28.9160(6)	11.3626(2)	8227.8(3)	514.03[d]	6.2	5.0
25	29.004(5)	11.317(5)	8245(4)	658.72	8.0	6.8
26	28.9152(18)	11.4141(8)	8264.7(14)	1036.55	12.5	9.5
27	28.3307(10)	11.5857(11)	8053.2(9)	1483.05	18.4	12.0
28	28.3778(6)	11.6370(3)	8115.8(3)	1214.66	15.0	11.4

[a]Calculated from the "smoothed solvent accessible surface", obtained from the Materials Studio program employing a spherical probe of 1.2 Å radius. Solvent molecules in the channels were removed before performing the calculations. Calculations of total solvent accessible surfaces give higher values but include small voids outside the channel region. [b]Estimated by calculating the "smoothed solvent accessible surface" using differing probe radii (increments/decrements of 0.05 Å). The value given is the diameter of the largest probe for which the calculation yields a continuous surface. [c]These values are slightly smaller than those reported in ref 17, due to a change in the method of calculation. [d]Ester group R^2 disordered over two positions. The minor component was removed before pore volume and diameter calculations. [e]Ester group R^2 disordered over two positions. A reasonable model of the crystal could be built using the assumption that R^2 in neighboring molecules occupied alternating positions, and this model was used for the pore volume and diameter calculations. [f]When the probe diameter is reduced to this value, voids are generated outside the channel region while a continuous pore surface has not yet appeared. [g]Ester group R^2 severely disordered and could not be located. [h]MeS disordered over two positions, one being removed before pore volume and diameter calculations.

iodobenzene (**26**). As illustrated in Figure 7, all are positioned where they can interact with guest molecules and participate in reactions or noncovalent interactions.

Finally, crystallography of acetamide **29** showed that not every molecule defined by Figure 3 adopts the $P6_1$ NPSU structure. In this case crystallization gave two polymorphs, depending on the solvent. A monoclinic ($P2_1$) form obtained from methyl acetate/water was denoted **29*α***, and a tetragonal ($P4_32_12_1$) form which crystallized from acetone/water was denoted **29*β***. The molecular units in the two forms are almost identical, and qualitatively different to those in the NPSUs; in particular, the C3 substituent is positioned so that the NH group points inward, creating a binding site which accommodates two water molecules (see Figures S31 and S32). In both crystals the packing is efficient, leaving no substantial voids (see Figures S57 and S58).

Crystal Porosity: Solvent Removal and Gas Adsorption. The term "nanoporous" implies that the crystal is permeable, allowing exchange of small guest molecules, and that this process does not substantially affect the host framework.[23] Ideally, the crystals should also be able to survive the removal of all guest molecules without loss of structure and then show reversible gas adsorption to confirm porosity.[11b] As mentioned earlier, we previously demonstrated that trifluoroacetamide **2** satisfies, at least, the guest-exchange criterion. The results from evacuation were less clear-cut; the powder XRD (PXRD) pattern remained essentially unchanged, but the crystals crazed and became opaque. However, further work established that **2** is atypical. Most NPSU crystals, especially those with 3α-ureido substituents, showed no change in appearance on evacuation. Nonetheless it was clearly desirable to establish the solvation state of a typical NPSU, show that the solvent could be removed, and demonstrate that the resulting crystals were unchanged and capable of gas adsorption. We chose tris-*N*-phenylurea **3** for this study, as this compound is the most accessible NPSU and has proved the most convenient for routine use.[19]

Crystals of **3** were obtained as needles from acetone/water (initial ratio 10:1), after washing with acetone and air-drying. Samples were then evacuated at room temperature and 100 °C for 24 h. The three samples (air-dried, RT evacuated, 100 °C evacuated) were then analyzed by ^{1}H NMR in DMSO, using a procedure which allowed the amount of background water to be measured and taken into account.[24] The crystals were also examined by light microscopy and PXRD. The composition of the air-dried crystals was found to be **3**:water:acetone = 1:3.8:0.2. Allowing for the single water molecule per steroid embedded in the channel wall, this implies that the pores are filled with ~3 molecules of H_2O per molecule of **3**, with a small amount of organic solvent also present. After evacuation at RT

dx.doi.org/10.1021/ja405701u | J. Am. Chem. Soc. 2013, 135, 16912−16925

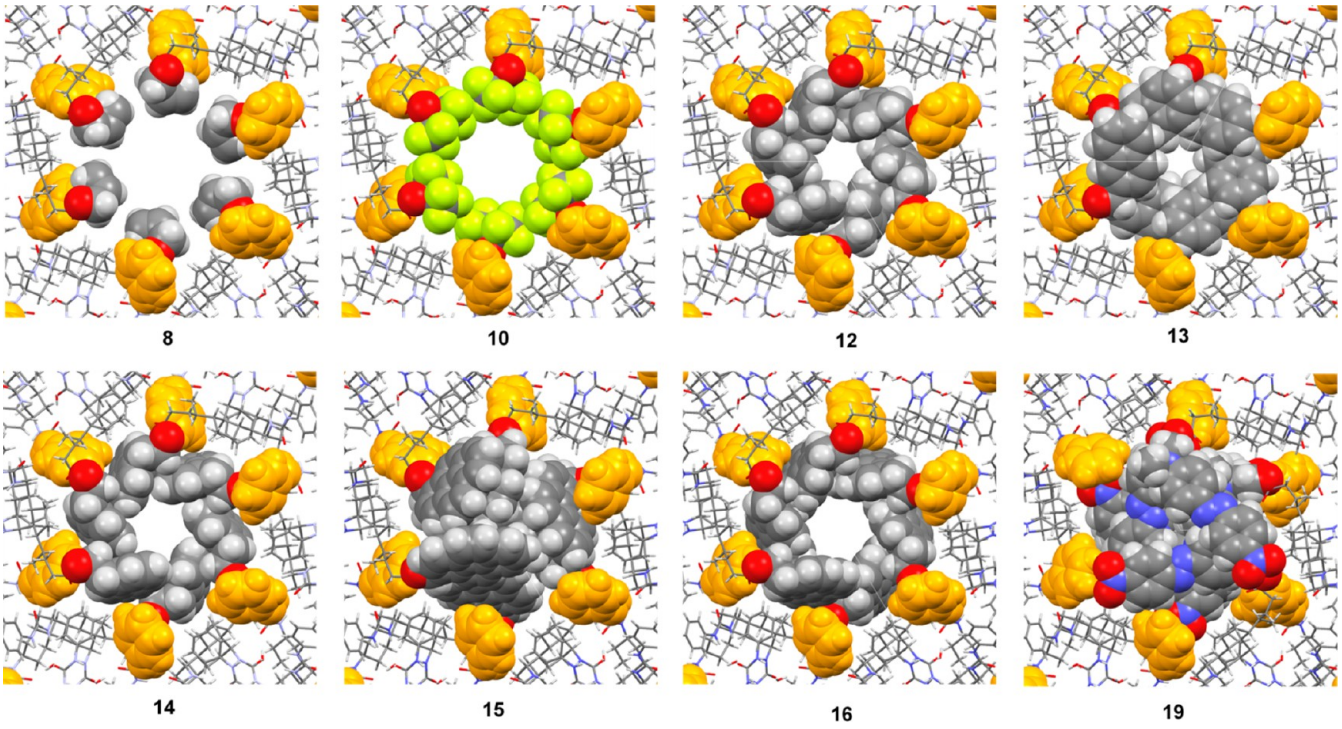

Figure 4. Channel regions of NPSU crystals from Chart 2, viewed along the channel axis. Terminal groups R^1 (= NHPh) and OR^2 are shown in space-filling mode, with R^1 colored gold. Some structures have been edited as indicated in Table 1.

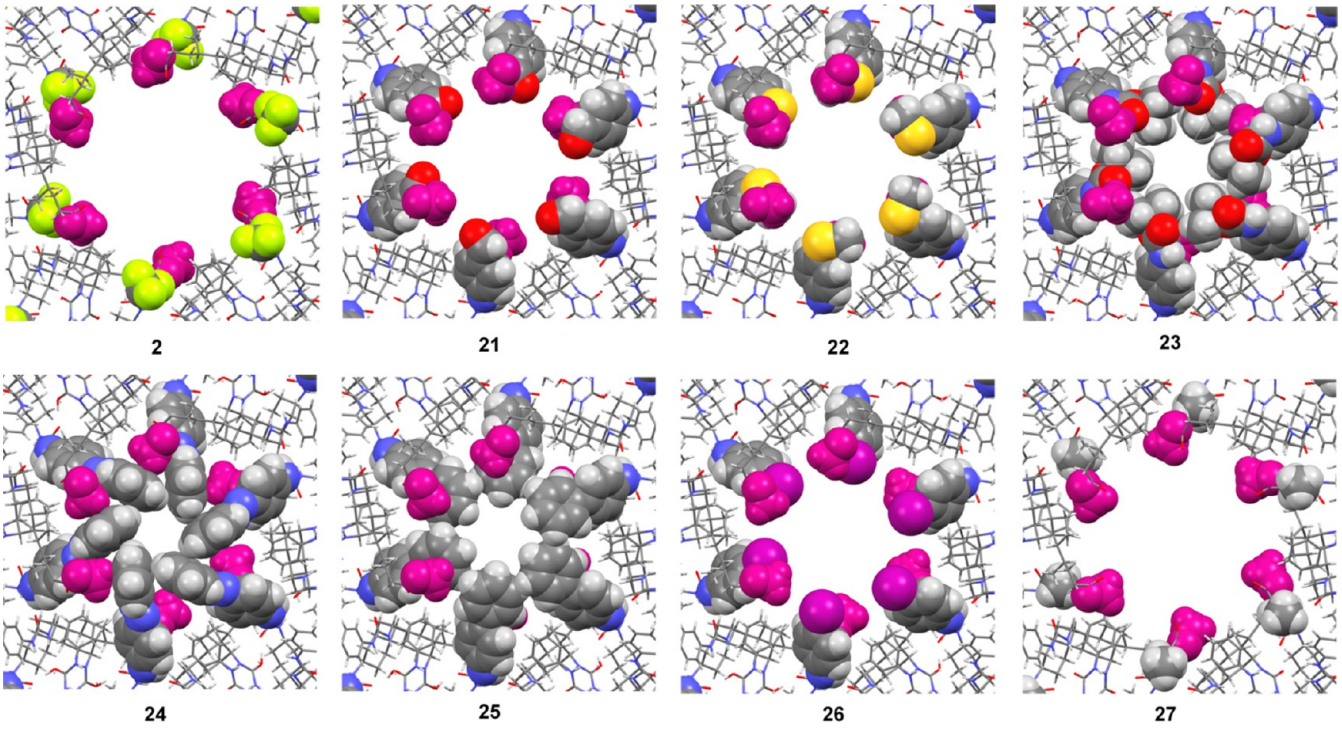

Figure 5. Channel regions of NPSU crystals from Chart 3, viewed along the channel axis. Terminal groups R^1 and OR^2 (= OMe) are shown in space-filling mode, with OR^2 colored magenta. Some structures have been edited as indicated in Table 1.

the composition was **3**:water = 1:1, implying that the channels are empty. Microscopy and PXRD revealed no significant changes. After evacuation at 100 °C for 24 h the ratio **3**:water reduced slightly to 1:0.9. This suggests some degradation, although microscopy and PXRD again showed no major changes. Samples of **3** were also heated to 150 °C and above, and in these cases clear signs of decomposition were observed both by microscopy (loss of transparency) and PXRD (loss of diffraction peaks).

Having established that the pores could be evacuated without loss of crystallinity, we proceeded to confirm the permanent porosity of **3** using N_2 gas adsorption measurements for a

dx.doi.org/10.1021/ja405701u | J. Am. Chem. Soc. 2013, 135, 16912−16925

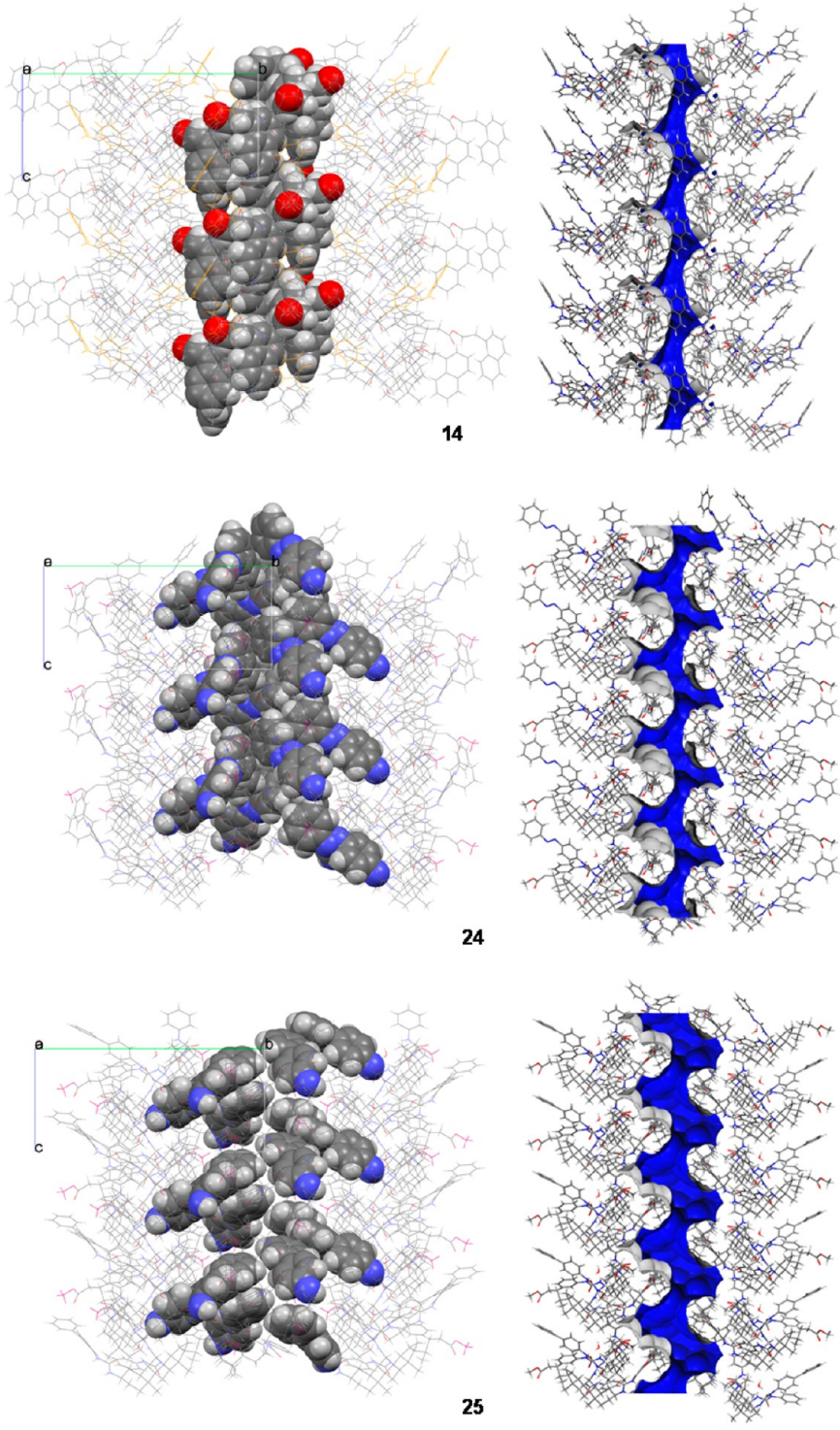

Figure 6. Crystal structures of **14**, **24**, and **25** viewed perpendicular to the *c* axis. For the images on the left, the groups which dominate the channel surface (OR^2 for **14**, R^1 for **24** and **25**) are highlighted in spacefilling mode. For the right-hand images, the smoothed solvent accessible surfaces have been added using Materials Studio, and the structures have then been sliced along the *c*-axis.

sample that had been heated under vacuum at 75 °C for 9 h. Surprisingly, the N_2 adsorption predominately takes place at high relative pressures (p/p^o > 0.7), and there is significant hysteresis between the adsorption and desorption isotherms giving a Type IV isotherm (see e.g., Figure 8).[25] This hysteresis differs from that observed in mesoporous materials (pore diameter >20 Å) that generally closes at lower relative pressures ($p/p_o \sim 0.4$) and which is related to pore evacuation involving capillary action. Furthermore, the desorption isotherm falls below that of the adsorption isotherm at $p/p_o \sim 0.7$. These unusual features are reproduced when the adsorption–desorption cycle is repeated and presumably reflect slow, nonequilibrium, kinetics of N_2 adsorption. Such slow kinetics is understandable if access to the pores is restricted to the relatively small number of openings located at the end of the long needle-shaped crystals, which are on average >2 mm in

dx.doi.org/10.1021/ja405701u | *J. Am. Chem. Soc.* 2013, 135, 16912–16925

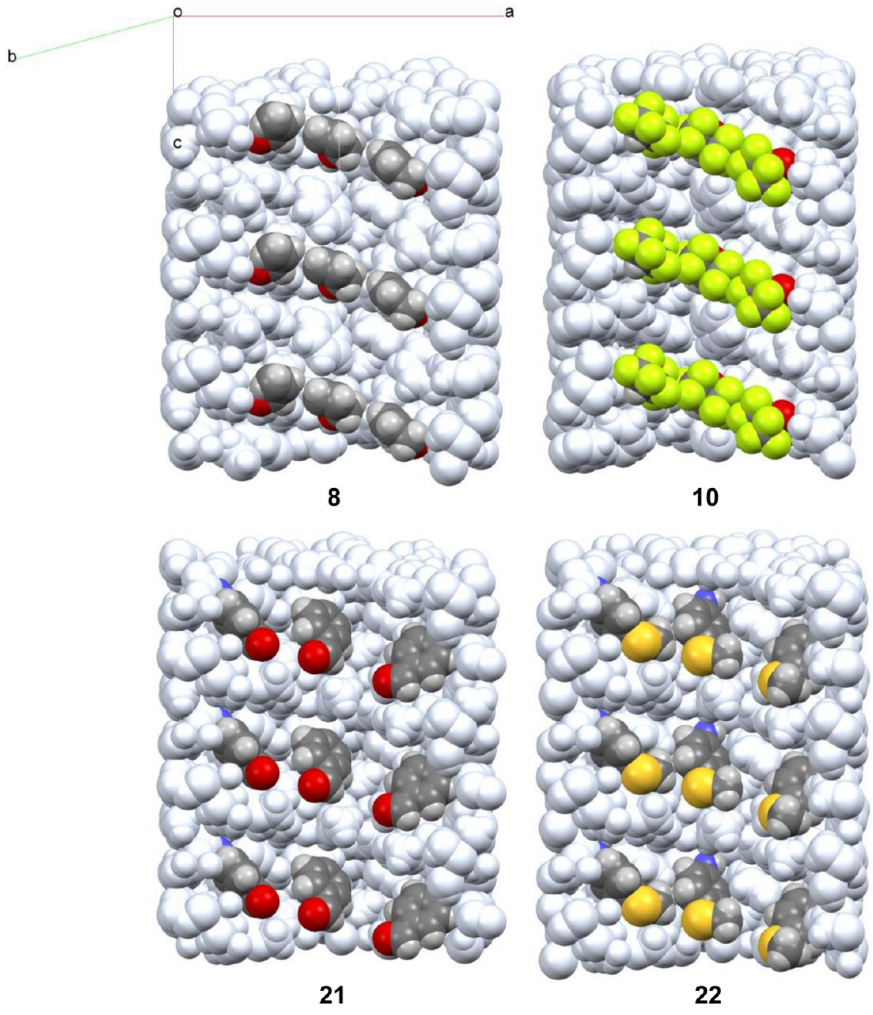

Figure 7. Space-filling representations of the channel regions in **8**, **10**, **21**, and **22**. The structures have been sliced along the *c*-axis to expose the pore interiors and are viewed roughly perpendicular to *c* and *a* (see axes attached to **8**). Conventional coloring is used for the distinctive groups in each structure (OR^2 for **8** and **10**, R^1 for **21** and **22**), the remaining atoms being shown as silver-blue. Some structures have been edited as indicated in Table 1.

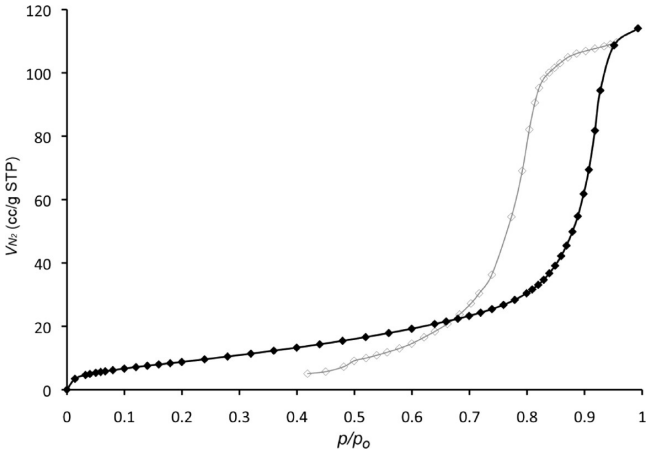

Figure 8. N_2 adsorption (◆) and desorption (◇) isotherms for crystal **3** at 77 K. See text for discussion.

length. We have previously shown that the pores in **3** are parallel to the long axis of the crystals.[17] Similar hysteresis was observed by Tosi-Pellenq et al. from the N_2 isotherms of long (150 μm) microporous crystals of $AlPO_4$-5,[26] which also contain cylindrical channels (0.76 nm in diameter) along the long axis of the crystals. In this case the hysteresis was attributed to delayed condensation of N_2 within the channels.[25] The fact that the desorption isotherm in Figure 8 dips below the adsorption isotherm implies that evaporating nitrogen is lost more rapidly from the channels than gaseous N_2 is readsorbed. This may relate to pressure differences between the interior and exterior of the crystals; it is reasonable to suppose that when the crystals are compressed, inward gas transfer could be relatively slow, while internal pressure could expand the crystals and assist N_2 efflux. The possibility that the effects are due to collapse of the crystal structure during N_2 analysis was discounted by confirming that the structure remained unchanged, as shown by SCXRD of a crystal extracted from the sample of **3** used for N_2 analysis.

The BET surface area calculated from the N_2 adsorption isotherm is very low (29 m^2/g) and probably represents only the external surface area of the crystals. However the pore volume of 0.17 mL/g calculated from the total N_2 uptake (4.9 mmol/g) is highly consistent with the guest-accessible volume (16.1%) calculated from the crystal structure (i.e., 0.17 mL/g equates to 16% of the total volume given a crystal framework density of 0.941 g/mL). The pore volume obtained from N_2

dx.doi.org/10.1021/ja405701u | J. Am. Chem. Soc. 2013, 135, 16912−16925

uptake is also consistent with the values calculated from the adsorption of liquid guests, as discussed in the following section.

Crystal Porosity: Adsorption of Organic Guest Molecules. NPSUs **2** and **3** were also studied as hosts for organic molecular guests. One series of experiments involved the liquid substrates **30**–**36** (Chart 4). Air-dried crystals of **3**

Chart 4. Organic Dyes Used for Adsorption Studies

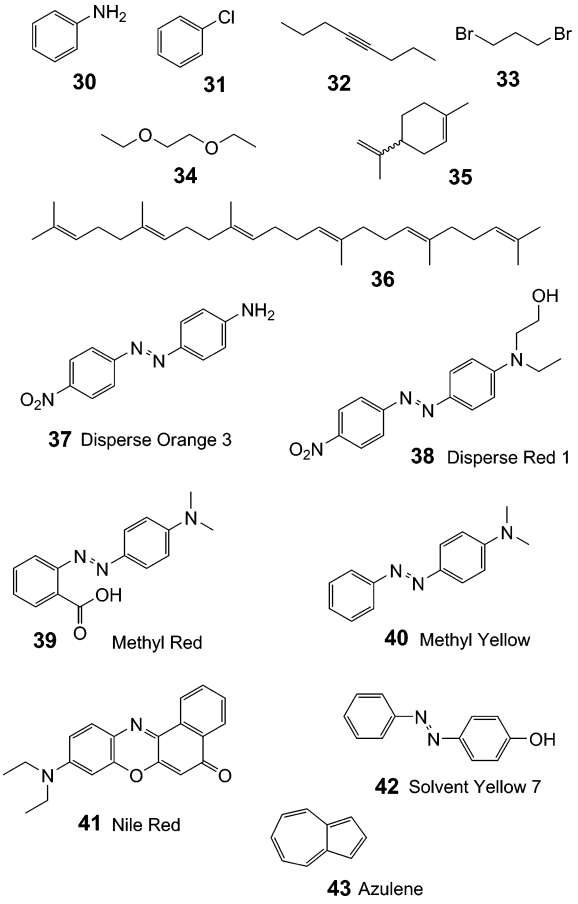

were placed in each, left for 12–24 h, washed briefly with ether, and subjected to ^{1}H NMR analysis. All of the substrates were adsorbed in significant amounts, as summarized in Table 2. Aniline **30** formed a well-defined host–guest 1:1 complex which could be characterized by X-ray crystallography. As shown in Figure 9, the aniline molecules form a helix within the

Table 2. Adsorption of Liquid Guests by NPSU 3

	amount adsorbed	
guest	equivalents	volume of liquid/mass of solid host (mL/g)[a]
aniline **30**	1	0.115
chlorobenzene **31**	1	0.128
oct-4-yne **32**	0.67	0.124
1,3-dibromopropane **33**	0.8	0.102
1,2-diethoxyethane **34**	0.4	0.071
limonene **35**	0.15	0.031
squalene **36**	0.14	0.084

[a]Calculated from guest/host mass ratio and density of liquid guest.

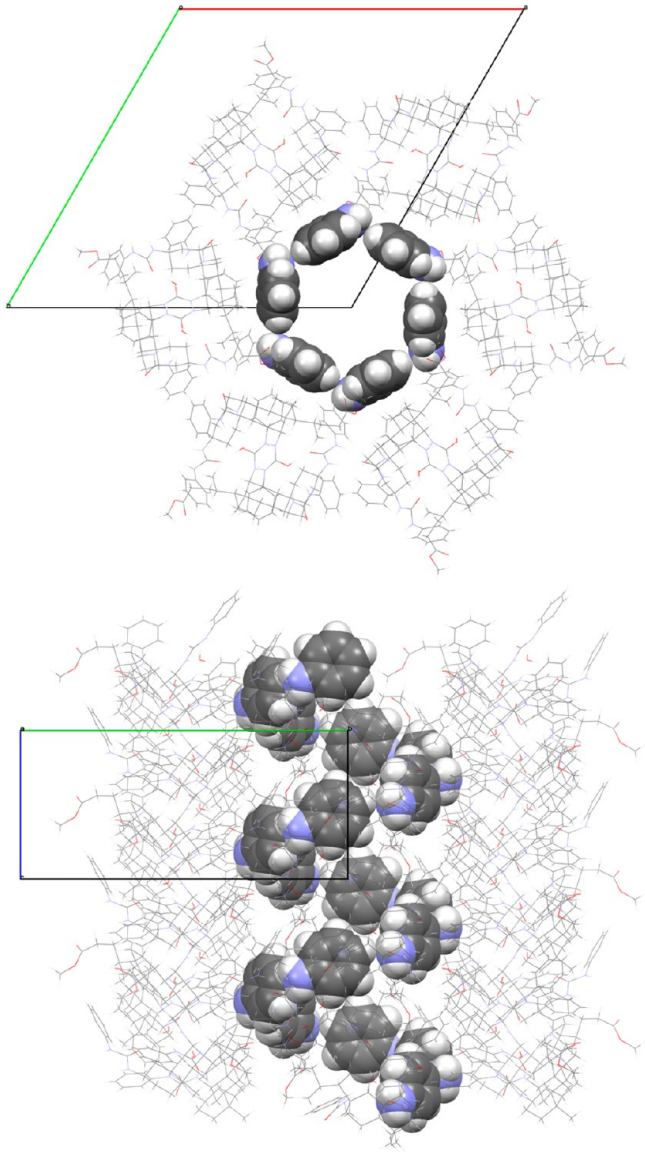

Figure 9. X-ray crystal structure of **3** with adsorbed aniline, viewed along the *c*-axis (top) and *a*-axis (bottom). The aniline is shown in space-filling mode.

channel, apparently stabilized by a close interguest CH···N contact ($d_{C-H\cdots N}$ = 2.68 Å). The anilines are also held in place by specific favorable interactions with the channel wall, including hydrogen bonds between amino NH and host ester carbonyl ($d_{N-H\cdots O}$ = 2.46 Å and $\theta_{N-H\cdots O}$ = 167.8°), NH–π interactions involving the second amino NH and a host phenyl group ($d_{N-H\cdots\pi}$ = 2.84 Å), and CH–π interactions to the aniline π-system. Chlorobenzene **31** was also absorbed in a 1:1 host–guest ratio, although in this case the guest could not be located crystallographically. Oct-4-yne **32** was taken up in a 3:2 host–guest ratio. For each of **30**–**32**, a calculation of the volume of liquid absorbed per unit mass of host gave a value of ∼0.12 mL/g, consistent with the pore volume obtained by gas adsorption (see above and Table 2). This represents a pore-filling efficiency of ∼70% using the pore volume calculated from the crystal structure, which is consistent with a strong affinity between the crystal and adsorbate.[27] Similar calculations based on the uptake of **33**–**36** suggested that these were absorbed less efficiently. However the value for squalene **36**, at

dx.doi.org/10.1021/ja405701u | J. Am. Chem. Soc. 2013, 135, 16912–16925

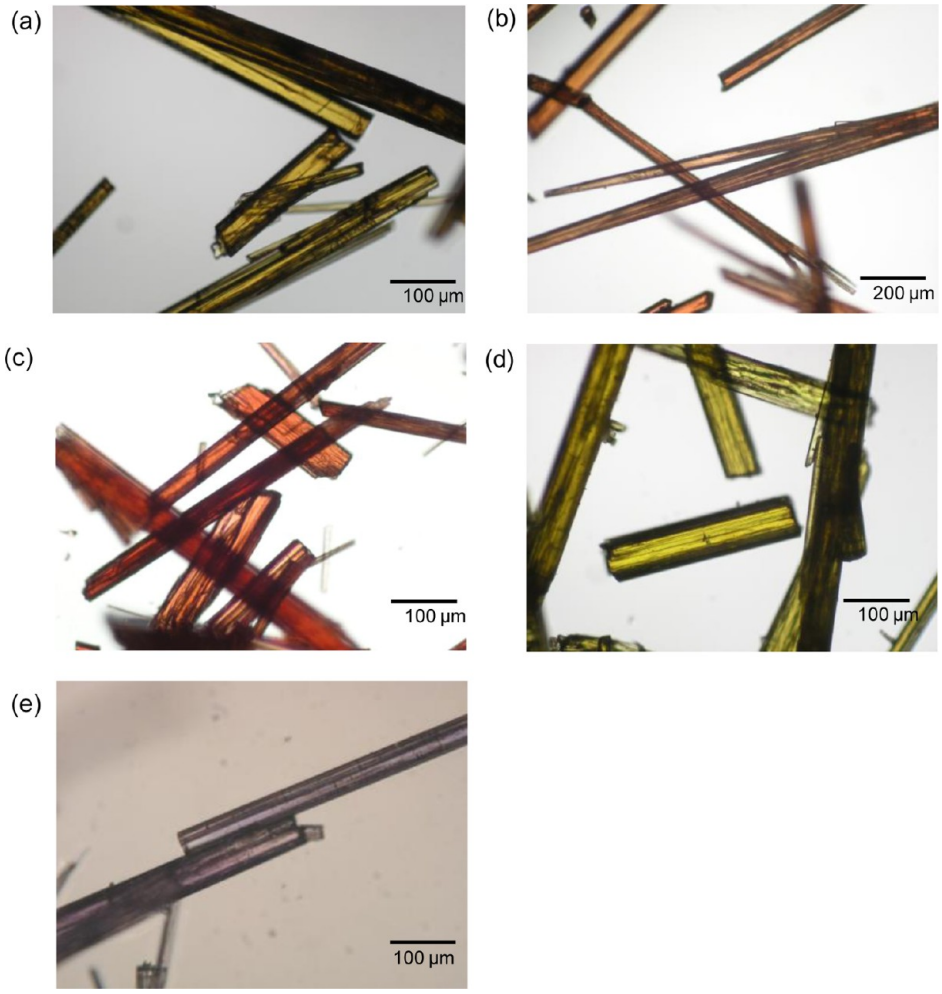

Figure 10. Crystals of **3** after exposure to ethereal solutions of (a) **37**, (b) **38**, (c) **39**, (d) **40**, and (e) **41**.

65% of the maximum, is remarkable for such a large (30-carbon) guest.

The aniline·**3** complex was used to investigate the kinetics of adsorption. Samples of air-dried crystalline **3** were place in aniline and then removed, washed with ether, and analyzed by ^{1}H NMR after periods ranging from 2 to 180 min. The results showed that the crystals are filled to about half capacity very quickly (within the first 2 min), but that subsequent adsorption is much slower. Saturation was reached after about 120 min. We were also interested to discover whether the aniline could be oxidized to polyaniline within the channels. Indeed, treatment of the complex with peroxyammonium sulfate in 0.1 N HCl caused the crystals to turn dark violet (after 4 h) then green (after 12 h). The diffuse-reflectance UV–vis spectrum of the product showed adsorption maxima at 420 and 795 nm consistent with polyaniline formation (see Figure S75).[28] PXRD analysis showed that the NPSU structure was retained, although the crystals were no longer suitable for single-crystal X-ray structure determination.

Another set of experiments involved the adsorption of larger guest molecules from solutions in diethyl ether. In these cases colored guests were used for ease of analysis and the potential for interesting or useful optical effects. The dyes employed are shown in Chart 4. In an initial screen, solutions of dyes **37**–**43** in ether (10–20 mM) were added to crystals of **3**, and the mixtures left to stand for 3 days. After isolation and washing with ether, all crystals were visibly colored. In the case of **37**–**41** the colors were strong enough to show clearly under a microscope (see Figure 10). As shown in Figure 10, the colors appeared to permeate the crystals and were not localized at ends or edges. Interestingly, the crystals containing Nile Red **41** were observed to be blue-purple (Figure 10e). This dye is strongly solvatochromic, its optical adsorption moving to longer wavelengths with increasing solvent polarity,[29] and a blue or purple color suggests a highly polar environment. Soaking the crystals in ether for 24 h resulted in loss of color, showing that the dye adsorption was reversible. A second NPSU crystal, trifluoroacetamide **2**, was also investigated as host and was found to absorb azo-dyes **37** and **38**. The combinations of **3** with Disperse Red 1 (**38**) and azulene (**43**) were investigated further, to establish how much dye was included and how fast. In the case of azulene, only ~1 mol % was absorbed, while equilibrium was reached within the first hour. In the case of **38**, the first 1 mol % was also absorbed quickly, but a further quantity (nearly 1 mol %) was taken up in a slower process over ~24 h.

Despite the appearance of the crystals there was room for concern that the dyes might not be entering the channels but somehow associated with cracks or defects in the crystals. To test this possibility, we examined the colored crystals under a microscope using plane polarized light. If the dyes were occupying the channels, it seemed likely that some (at least)

would show preferential alignments. If the transition dipole moments were to lie roughly along the channel axis (the long axis of the crystal) the crystals should be dichroic, i.e., their colors should be dependent on their orientation with respect to the plane of polarization. We were pleased to find that this was true for several combinations. Figure 11 shows pairs of

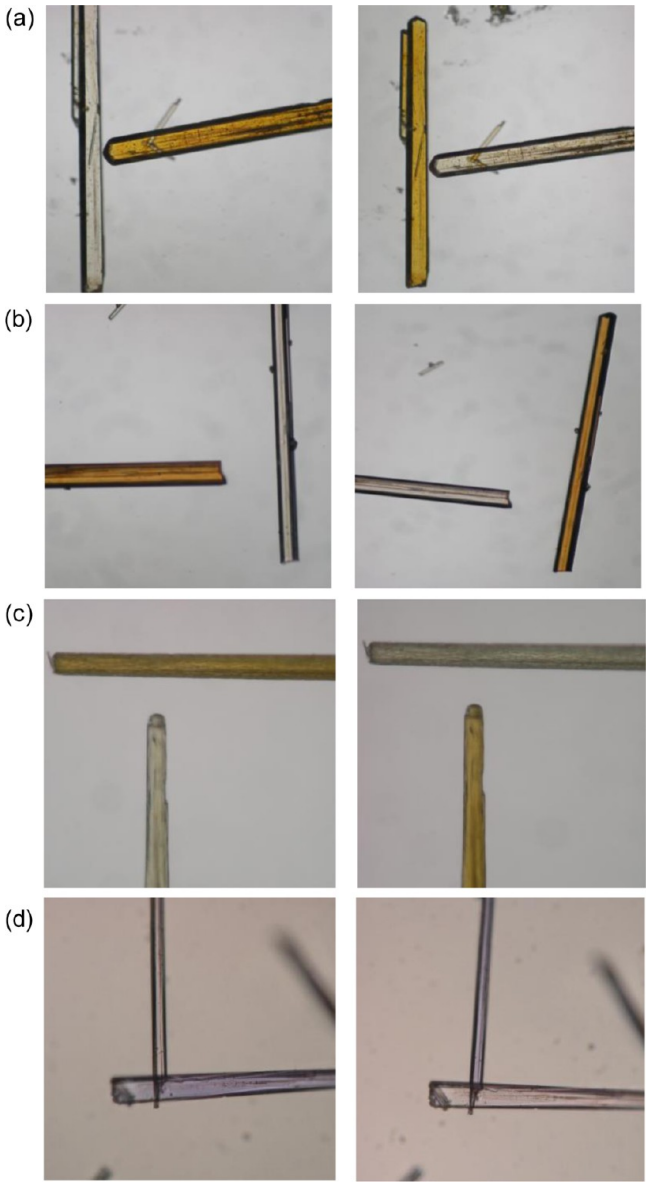

Figure 11. Crystals of NPSUs with included dyes illuminated with polarized light. For each pair of images the plane of polarization is rotated through 90° between left and right. (a) **2**·**37**, (b) **2**·**38**, (c) **3**·**37**, (d) **3**·**41**.

photomicrographs in which crystals of identical composition, but oriented at roughly 90° to each other, are illuminated with polarized light. Each pair of images shows the same crystals, with the plane of polarization differing by 90°. The crystals are clearly dichroic, changing from colored to almost colorless as the plane of polarization is rotated. The effect was observed for **2**·**37**, **2**·**38**, **3**·**37**, **3**·**38**, and **3**·**41** but not for **3**·**39** or **3**·**40**. The guests which lead to dichroism (**37**, **38**, and **41**) possess extended dipoles due to conjugation of an amino group with an electron acceptor. This feature should encourage the molecules to adopt a head-to-tail arrangement parallel to the channel axis. The images in Figure 11 provide strong evidence that the dye molecules are indeed in the channels revealed by crystallography.

It should be noted that this phenomenon of dye uptake by organic molecular crystals is rare and may be unprecedented. It is well-known that dyes may be adsorbed by inorganic crystals, such as zeolites,[30] or by organic–inorganic hybrids (PCPs/MOFs).[31] However, the inclusion of dyes in organic molecular crystals is normally achieved by cocrystallization,[6,32,33] not by the interaction of substrates with macroscopically sized preformed crystals. This ability of NPSUs to adsorb such large guest molecules highlights their unusual combination of robust crystal structures with spacious accessible interiors.

CONCLUSION

In principle, the NPSU crystal packing represents a powerful tool for the design of functional materials. Whether that potential can be realized depends largely on two factors. First, the structure needs to be generalizable, forming in (at least) most of the cases where it might be predicted. Second, the crystals need to be truly porous so that the space within may be exploited. This work provides reassurance on both counts. We have now examined the crystal structures of 26 molecules with the general structure represented in Figure 3, and of these only one (acetamide **29**) fails to adopt the $P6_1$ NPSU arrangement. The range of NPSUs now includes examples with vanishingly small pores sizes, strongly corrugated pore surfaces, and several cases with potentially reactive functional groups ($CH_2CH{=}CH_2$ in **8**, CH=O in **21**, SMe in **22**, and NHBoc in **23**). It is notable that neither the aldehyde nor NHBoc groups, both of which are quite polar, disturbed the NPSU packing. We have also shown that the pores can be evacuated without loss of integrity and that subsequent gas adsorption is possible (although given the pressures involved and the low pore volume, applications in gas storage are unrealistic). More importantly, organic molecules are also absorbed, including the large rigid Nile Red **41** (M_w 318), and the even larger but more flexible squalene **36** (M_w 411). The ability to orient dye molecules suggests applications in display technology and nonlinear optics. Although not all dyes showed this behavior, the tunability of the pores implies that the phenomenon should be extendable (e.g., by tailoring of channel diameter). The fact that small molecules can readily access the pores points to further applications in catalysis, sensing, and separations, especially given the chirality of the crystals and the ability to incorporate effector groups through alloy formation.[19] We hope to explore these and other possibilities in future work.

ASSOCIATED CONTENT

Supporting Information

Experimental procedures and the characterization data for all new compounds; details of crystallography, including molecular structures (Figures S12–S33) and crystal packing diagrams with solvent accessible surfaces (Figures S34–S58); experimental details for studies of inclusion behavior, including NMR spectra and photographs of solvent-free host **3** and its inclusion complexes. This material is available free of charge via the Internet at http://pubs.acs.org.

AUTHOR INFORMATION

Corresponding Author

Anthony.Davis@bristol.ac.uk

Present Address

[#]Chemistry Division, CSIR-Indian Institute of Chemical Biology, Kolkata 700032, India.

Notes

The authors declare no competing financial interest.

■ ACKNOWLEDGMENTS

This work was supported by the EPSRC (EP/E021581/1 and EP/H024034/1) and Naresuan University, Thailand (Fellowship to A. S.). L. B. is a member of the Bristol Centre for Functional Nanomaterials, an EPSRC-funded Doctoral Training Centre.

■ REFERENCES

(1) (a) Hollingsworth, M. D. *Science* **2002**, *295*, 2410−2413. (b) Desiraju, G. R. *Angew. Chem., Int. Ed.* **2007**, *46*, 8342−8356. (c) Desiraju, G. R.; Vittal, J. J.; Ramanan, A. *Crystal Engineering*; World Scientific Publishing Co.: Singapore, 2011.

(2) Woodley, S. M.; Catlow, R. *Nat. Mater.* **2008**, *7*, 937−946.

(3) (a) Desiraju, G. R. *Angew. Chem., Int. Ed. Engl.* **1995**, *34*, 2311−2327. (b) Yaghi, O. M.; O'Keeffe, M.; Ockwig, N. W.; Chae, H. K.; Eddaoudi, M.; Kim, J. *Nature* **2003**, *423*, 705−714. (c) Wuest, J. D. *Chem. Commun.* **2005**, 5830−5837. (d) Cruz-Cabeza, A. J.; Day, G. M.; Jones, W. *Chem.—Eur. J.* **2009**, *15*, 13033−13040.

(4) (a) Rowsell, J. L. C.; Yaghi, O. M. *Angew. Chem., Int. Ed.* **2005**, *44*, 4670−4679. (b) Lim, S.; Kim, H.; Selvapalam, N.; Kim, K. J.; Cho, S. J.; Seo, G.; Kim, K. *Angew. Chem., Int. Ed.* **2008**, *47*, 3352−3355. (c) Kim, H.; Kim, Y.; Yoon, M.; Linn, S.; Park, S. M.; Seo, G.; Kim, K. *J. Am. Chem. Soc.* **2010**, *132*, 12200−12202. (d) Jin, Y. H.; Voss, B. A.; Noble, R. D.; Zhang, W. *Angew. Chem., Int. Ed.* **2010**, *49*, 6348−6351. (e) Mastalerz, M.; Schneider, M. W.; Oppel, I. M.; Presly, O. *Angew. Chem., Int. Ed.* **2011**, *50*, 1046−1051. (f) Sozzani, P.; Bracco, S.; Comotti, A.; Ferretti, L.; Simonutti, R. *Angew. Chem., Int. Ed.* **2005**, *44*, 1816−1820. (g) Comotti, A.; Bracco, S.; Distefano, G.; Sozzani, P. *Chem. Commun.* **2009**, 284−286. (h) Yang, W. B.; Greenaway, A.; Lin, X. A.; Matsuda, R.; Blake, A. J.; Wilson, C.; Lewis, W.; Hubberstey, P.; Kitagawa, S.; Champness, N. R.; Schroder, M. *J. Am. Chem. Soc.* **2010**, *132*, 14457−14469.

(5) (a) Herbstein, F. H. *Crystalline Molecular Complexes and Compounds*; Oxford University Press: Oxford, 2005. (b) Shimizu, L. S.; Hughes, A. D.; Smith, M. D.; Davis, M. J.; Zhang, B. P.; zur Loye, H. C.; Shimizu, K. D. *J. Am. Chem. Soc.* **2003**, *125*, 14972−14973. (c) Wang, X.; Simard, M.; Wuest, J. D. *J. Am. Chem. Soc.* **1994**, *116*, 12119−12120. (d) Brunet, P.; Simard, M.; Wuest, J. D. *J. Am. Chem. Soc.* **1997**, *119*, 2737−2738.

(6) (a) Hoss, R.; Konig, O.; KramerHoss, V.; Berger, U.; Rogin, P.; Hulliger, J. *Angew. Chem., Int. Ed. Engl.* **1996**, *35*, 1664−1666. (b) Botta, C.; Patrinoiu, G.; Picouet, P.; Yunus, S.; Communal, J. E.; Cordella, F.; Quochi, F.; Mura, A.; Bongiovanni, G.; Pasini, M.; Destri, S.; Di Silvestro, G. *Adv. Mater.* **2004**, *16*, 1716−1721.

(7) (a) Yang, J.; Dewal, M. B.; Shimizu, L. S. *J. Am. Chem. Soc.* **2006**, *128*, 8122−8123. (b) Yang, J.; Dewal, M. B.; Profeta, S.; Smith, M. D.; Li, Y. Y.; Shimizu, L. S. *J. Am. Chem. Soc.* **2008**, *130*, 612−621. (c) Dawn, S.; Dewal, M. B.; Sobransingh, D.; Paderes, M. C.; Wibowo, A. C.; Smith, M. D.; Krause, J. A.; Pellechia, P. J.; Shimizu, L. S. *J. Am. Chem. Soc.* **2011**, *133*, 7025−7032. (d) Ikemoto, K.; Inokuma, Y.; Fujita, M. *Angew. Chem., Int. Ed.* **2010**, *49*, 5750−5752. (e) Inokuma, Y.; Kojima, N.; Arai, T.; Fujita, M. *J. Am. Chem. Soc.* **2011**, *133*, 19691−19693. (f) Endo, K.; Koike, T.; Sawaki, T.; Hayashida, O.; Masuda, H.; Aoyama, Y. *J. Am. Chem. Soc.* **1997**, *119*, 4117−4122.

(8) (a) *Separations and Reactions in Organic Supramolecular Chemistry: Perspectives in Supramolecular Chemistry*; Toda, F.; Bishop. R., Ed; John Wiley & Sons Ltd: Chichester, 2004, Vol. *8*. (b) Moorthy, J. N.; Natarajan, P.; Venugopalan, P. *J. Org. Chem.* **2009**, *74*, 8566−8577. (c) Afonso, R. V.; Durao, J.; Mendes, A.; Damas, A. M.; Gales, L. *Angew. Chem., Int. Ed.* **2010**, *49*, 3034−3036. (d) Bloch, E. D.; Queen, W. L.; Krishna, R.; Zadrozny, J. M.; Brown, C. M.; Long, J. R. *Science* **2012**, *335*, 1606−1610.

(9) (a) Bradshaw, D.; Prior, T. J.; Cussen, E. J.; Claridge, J. B.; Rosseinsky, M. J. *J. Am. Chem. Soc.* **2004**, *126*, 6106−6114. (b) Vaidhyanathan, R.; Bradshaw, D.; Rebilly, J. N.; Barrio, J. P.; Gould, J. A.; Berry, N. G.; Rosseinsky, M. J. *Angew. Chem., Int. Ed.* **2006**, *45*, 6495−6499.

(10) (a) Bradshaw, D.; Claridge, J. B.; Cussen, E. J.; Prior, T. J.; Rosseinsky, M. J. *Acc. Chem. Res.* **2005**, *38*, 273−282. (b) Kitagawa, S.; Kitaura, R.; Noro, S. *Angew. Chem., Int. Ed.* **2004**, *43*, 2334−2375. (c) Lin, W. B.; Rieter, W. J.; Taylor, K. M. L. *Angew. Chem., Int. Ed.* **2009**, *48*, 650−658. (d) Kepert, C. J. *Chem. Commun.* **2006**, 695−700. (e) Robson, R. *Dalton Trans.* **2008**, 5113−5131. (f) Long, J. R.; Yaghi, O. M. *Chem. Soc. Rev.* **2009**, *38*, 1213−1214.

(11) (a) Holst, J. R.; Trewin, A.; Cooper, A. I. *Nat. Chem.* **2010**, *2*, 915−920. (b) McKeown, N. B. *J. Mater. Chem.* **2010**, *20*, 10588−10597. (c) Couderc, G.; Hulliger, J. *Chem. Soc. Rev.* **2010**, *39*, 1545−1554. (d) Tian, J.; Thallapally, P. K.; McGrail, B. P. *CrystEngComm* **2012**, *14*, 1909−1919.

(12) Leading references: (a) Jones, J. T. A.; Hasell, T.; Wu, X.; Bacsa, J.; Jelfs, K. E.; Schmidtmann, M.; Chong, S. Y.; Adams, D. J.; Trewin, A.; Schiffman, F.; Cora, F.; Slater, B.; Steiner, A.; Day, G. M.; Cooper, A. I. *Nature* **2011**, *474*, 367−371. (b) Tozawa, T.; Jones, J. T. A.; Swamy, S. I.; Jiang, S.; Adams, D. J.; Shakespeare, S.; Clowes, R.; Bradshaw, D.; Hasell, T.; Chong, S. Y.; Tang, C.; Thompson, S.; Parker, J.; Trewin, A.; Bacsa, J.; Slawin, A. M. Z.; Steiner, A.; Cooper, A. I. *Nat. Mater.* **2009**, *8*, 973−978. (c) Hasell, T.; Schmidtmann, M.; Cooper, A. I. *J. Am. Chem. Soc.* **2011**, *133*, 14920−14923. (d) Brea, R. J.; Reiriz, C.; Granja, J. R. *Chem. Soc. Rev.* **2010**, *39*, 1448−1456. (e) Brea, R. J.; Castedo, L.; Granja, J. R. *Chem. Commun.* **2007**, 3267−3269. (f) Thallapally, P. K.; McGrail, B. P.; Dalgarno, S. J.; Schaef, H. T.; Tian, J.; Atwood, J. L. *Nat. Mater.* **2008**, *7*, 146−150. (g) Fritzsche, M.; Bohle, A.; Dudenko, D.; Baumeister, U.; Sebastiani, D.; Richardt, G.; Spiess, H. W.; Hansen, M. R.; Hoger, S. *Angew. Chem., Int. Ed.* **2011**, *50*, 3030−3033. (h) Gauthier, D.; Baillargeon, P.; Drouin, M.; Dory, Y. L. *Angew. Chem., Int. Ed.* **2001**, *40*, 4635−4638.

(13) (a) Harris, K. D. M. *Chem. Soc. Rev.* **1997**, *26*, 279−289. (b) Marti-Rujas, J.; Desmedt, A.; Harris, K. D. M.; Guillaume, F. *J. Am. Chem. Soc.* **2004**, *126*, 11124−11125. (c) Marti-Rujas, J.; Desmedt, A.; Harris, K. D. M.; Guillaume, F. *J. Phys. Chem. C* **2009**, *113*, 736−743.

(14) (a) Gorbitz, C. H. *Chem.—Eur. J.* **2001**, *7*, 5153−5159. (b) Gorbitz, C. H. *Chem.—Eur. J.* **2007**, *13*, 1022−1031. (c) Soldatov, D. V.; Moudrakovski, I. L.; Ripmeester, J. A. *Angew. Chem., Int. Ed.* **2004**, *43*, 6308−6311. (d) Soldatov, D. V.; Moudrakovski, I. L.; Grachev, E. V.; Ripmeester, J. A. *J. Am. Chem. Soc.* **2006**, *128*, 6737−6744. (e) Endo, K.; Sawaki, T.; Koyanagi, M.; Kobayashi, K.; Masuda, H.; Aoyama, Y. *J. Am. Chem. Soc.* **1995**, *117*, 8341−8352. (f) Brunet, P.; Demers, E.; Maris, T.; Enright, G. D.; Wuest, J. D. *Angew. Chem., Int. Ed.* **2003**, *42*, 5303−5306. (g) Malek, N.; Maris, T.; Perron, M.-E.; Wuest, J. D. *Angew. Chem., Int. Ed.* **2005**, *44*, 4021−4025. (h) Mansikkamaki, H.; Nissinen, M.; Rissanen, K. *Angew. Chem., Int. Ed.* **2004**, *43*, 1243−1246. (i) Mansikkamaki, H.; Busi, S.; Nissinen, M.; Ahman, A.; Rissanen, K. *Chem.—Eur. J.* **2006**, *12*, 4289−4296. (j) Carrasco, H.; Foces-Foces, C.; Perez, C.; Rodriguez, M. L.; Martin, J. D. *J. Am. Chem. Soc.* **2001**, *123*, 11970−11981. (l) Febles, M.; Perez-Hernandez, N.; Perez, C.; Rodriguez, M. L.; Foces-Foces, C.; Roux, M. V.; Morales, E. Q.; Buntkowsky, G.; Limbach, H. H.; Martin, J. D. *J. Am. Chem. Soc.* **2006**, *128*, 10008−10009. (m) Mastalerz, M.; Oppel, I. M. *Angew. Chem., Int. Ed.* **2012**, *51*, 5232−5255. (n) Msayib, K. J.; Book, D.; Budd, P. M.; Chaukura, N.; Harris, K. D. M.; Helliwell, M.; Tedds, S.; Walton, A.; Warren, J. E.; Xu, M. C.; McKeown, N. B. *Angew. Chem., Int. Ed.* **2009**, *48*, 3273−3277. (m) Pantos, G. D.; Pengo, P.; Sanders, J. K. M. *Angew. Chem., Int. Ed.* **2007**, *46*, 194−197.

(15) A notable example is provided by the dipeptides studied by Görbitz, Soldatov, Ripmeester, and others; see refs 14a−d. However even in this case, the variations possible within a single packing motif are relatively narrow.

(16) (a) Valkenier, H.; Davis, A. P. *Acc. Chem. Res.* **2013**, DOI: 10.1021/ar4000345. (b) Brotherhood, P. R.; Davis, A. P.

Chem. Soc. Rev. **2010**, *39*, 3633−3647. (c) Davis, A. P. *Coord. Chem. Rev.* **2006**, *250*, 2939−2951. (d) Davis, A. P.; Joos, J.-B. *Coord. Chem. Rev.* **2003**, *240*, 143−156.
(17) Sisson, A. L.; del Amo Sanchez, V.; Magro, G.; Griffin, A. M. E.; Shah, S.; Charmant, J. P. H.; Davis, A. P. *Angew. Chem., Int. Ed.* **2005**, *44*, 6878−6881.
(18) Natarajan, R.; Charmant, J. P. H.; Orpen, A. G.; Davis, A. P. *Angew. Chem., Int. Ed.* **2010**, *49*, 5125−5129.
(19) Natarajan, R.; Magro, G.; Bridgland, L. N.; Sirikulkajorn, A.; Narayanan, S.; Ryan, L. E.; Haddow, M. F.; Orpen, A. G.; Charmant, J. P. H.; Hudson, A. J.; Davis, A. P. *Angew. Chem., Int. Ed.* **2011**, *50*, 11386−11390. See also Mastalerz, M. *Angew. Chem., Int. Ed.* **2012**, *51*, 584−586.
(20) del Amo, V.; Siracusa, L.; Markidis, T.; Baragana, B.; Bhattarai, K. M.; Galobardes, M.; Naredo, G.; Perez-Payan, M. N.; Davis, A. P. *Org. Biomol. Chem.* **2004**, *2*, 3320−3328.
(21) del Amo, V.; Bhattarai, K.; Nissinen, M.; Rissanen, K.; Pérez-Payán, M. N.; Davis, A. P. *Synlett* **2005**, 1319−1321.
(22) McNally, B. A.; Koulov, A. V.; Lambert, T. N.; Smith, B. D.; Joos, J. B.; Sisson, A. L.; Clare, J. P.; Sgarlata, V.; Judd, L. W.; Magro, G.; Davis, A. P. *Chem.—Eur. J.* **2008**, *14*, 9599−9606.
(23) Barbour, L. J. *Chem. Commun.* **2006**, 1163−1168.
(24) For details, see Supporting Information
(25) Rouquerol, F.; Rouquerol, J.; Sing, K. *Adsorption by Powders and Porous Solids*; AP: New York, 1999, p 427.
(26) Tosi-Pellenq, N.; Grillet, Y.; Rouquerol, J.; Llewellyn, P. *Thermochim. Acta* **1992**, *204*, 79−88.
(27) Mecozzi, S.; Rebek, J. *Chem.—Eur. J.* **1998**, *4*, 1016−1022.
(28) (a) Liu, Y.; Shi, J.; Chen, Y.; Ke, C. F. *Angew. Chem., Int. Ed.* **2008**, *47*, 7293−7296. (b) Surwade, S. P.; Agnihotra, S. R.; Dua, V.; Manohar, N.; Jain, S.; Ammu, S.; Manohar, S. K. *J. Am. Chem. Soc.* **2009**, *131*, 12528−12529.
(29) Deye, J. F.; Berger, T. A.; Anderson, A. G. *Anal. Chem.* **1990**, *62*, 615−622.
(30) (a) Calzaferri, G.; Huber, S.; Maas, H.; Minkowski, C. *Angew. Chem., Int. Ed.* **2003**, *42*, 3732−3758. (b) Calzaferri, G.; Li, H. R.; Bruhwiler, D. *Chem.—Eur. J.* **2008**, *14*, 7442−7449. (c) *Host-guest systems based on nanoporous crystals*; Laeri, F.; Schuth, F.; Simon, U.; Wark, M., Eds.; Wiley-VCH: Weinheim, 2003.
(31) Yu, J. C.; Cui, Y. J.; Wu, C. D.; Yang, Y.; Wang, Z. Y.; O'Keeffe, M.; Chen, B. L.; Qian, G. D. *Angew. Chem., Int. Ed.* **2012**, *51*, 10542−10545.
(32) Sozzani, P.; Comotti, A.; Bracco, S.; Simonutti, R. *Angew. Chem., Int. Ed.* **2004**, *43*, 2792−2797.
(33) Soegiarto, A. C.; Comotti, A.; Ward, M. D. *J. Am. Chem. Soc.* **2010**, *132*, 14603−14616.